# SECOND ORDER NUMERICAL SOLUTION FOR OPTIMAL CONTROL OF MONODOMAIN MODEL IN CARDIAC ELECTROPHYSIOLOGY

CHAMAKURI NAGAIAH, KARL KUNISCH * AND GERNOT PLANK †

**Abstract.** In this article, second order numerical methods for optimal control of the monodomain equations in cardiac electrophysiology are presented. The mono- and bidomain equations are well established as a major building block for describing the the wave propagation of the action potential in the human heart. The mathematical model equations consist of a non-linear parabolic partial differential equation of reaction-diffusion type, coupled with ordinary differential equations describing the interaction with the ionic current variables. Optimal control problems suggest themselves quite naturally for this important class of modeling problems. Specifically we present an optimal control formulation for the monodomain equations with an extra-cellular current as the control variable which must be determined in such a way that excitations of the transmembrane voltage are damped in an optimal manner. A nonlinear conjugate gradient method and a Newton method are compared for solving the optimization problem.

**Key words.** Reaction-diffusion systems, optimal control problems, constrained PDE's.

**AMS subject classifications.** 35J55, 35K57, 49J20, 74S05

**1. Introduction.** Modeling the bioelectrical activity of the action potential in the cardiac domain and the corresponding numerical realization have received a significant amount of attention in the last decade. Previous studies focused on important issues such as wave propagation of the action potential, development of spiral waves and effects of strong electrical shocks such as cardiac arrhythmias. A well established mathematical model is the bidomain model which consisting of a system of reaction-diffusion equations coupled with stiff ordinary differential equations. In the numerical simulations there are many important factors which put a high demand on the computing time such as different length and time scales of the reaction terms, strong nonlinearities caused by ionic currents, anisotropy related to the fiber orientation, and rapid changes of the potentials. We have chosen the finite element method for the spatial and higher order linearly implicit Runge-Kutta time stepping methods for the temporal discretization.

Due to cardiac arrhythmia the heart beat may be slow or fast and regular or irregular. For the optimal control of cardiac arrhythmia system, it is essential to determine the control response of an electrical field, which can be realized by an implanted defibrillator, which is able to drive the system from a arrhythmia pattern to a uniform pattern. Also, it is important to determine the optimal transmembrane current density in such a way that it dampens the gradients of the electrical voltage in the system. The present article is devoted to the numerical solution of the optimal control for monodomain equations.

The optimal control approach is based on minimizing a properly chosen cost functional $J(V_m, I_e)$ depending on the extracellular current $I_e$ as input and on the

---

*Institute of Mathematics and Scientific Computing, University of Graz, Heinrichstr. 36, Graz, A-8010, Austria (`nagaiah.chamakuri@uni-graz.at, karl.kunisch@uni-graz.at`).

†Institute of Biophysics, Medical University of Graz, Harrachgasse 21, Graz, A-8010, Austria (`gernot.plank@meduni-graz.at`).

transmembrane potential $V_m$ as one of the state variables.

The organization of this article as follows: in the next section the governing equations for the action potential and the behavior of the ionic current variables using ionic models are described. In section 3 the control problem is posed for the monodomain equations and the optimality system is derived. Section 4 contains the description of the numerical approach to solve the primal and the adjoint state equations and the optimization problem. Numerical results for two test cases are presented in section 5. Finally concluding remarks are given.

**2. The monodomain equations.** The most complete description of cardiac electricity is given by the bidomain equations. The bidomain model consists of the equations for the extracellular potential and the transmembrane potential. We refer to [12, 4] for more detailed derivation of bidomain model and further discussions. Moreover, the numerical simulation of bidomain equations are very expensive compared to the monodomain models because they require the solution of a system of linear equations at each time step. Moreover, to solve accurately the complete cardiac domain requires a fine numerical discretization. In such cases monodomain models are alternative to reduce the computational time which are more comparable with bidomain models, see for more details Potse et.al. [13]. Also in [10] Nielsen et.al. formulated a parameter estimation problem for the monodomain equation. Its objective is to approximate the bidomain - by a monodomain equation by appropriate fitting of the scalar coefficient in the latter.

We set $Q_c = \Omega_c \times [0, t_f]$ where $\Omega_c$ denotes the cardiac tissue sample domain.

$$(2.1) \qquad \nabla \cdot \bar{\sigma}_i \nabla V_m = \beta \left( C_m \frac{\partial V_m}{\partial t} + I_{ion}(V_m, v) - I_e \right) \quad \text{in } Q_c$$

$$(2.2) \qquad \frac{\partial v}{\partial t} = g(V_m, v) \quad \text{in } Q_c$$

where $V_m : Q_c \to \mathrm{R}$ is the transmembrane voltage, $v : Q_c \to \mathrm{R}^n$ represents the ionic current variables, $\bar{\sigma}_i : \Omega_c \to \mathrm{R}^{d \times d}$ is the intracellular conductivity tensors, $\beta$ is the surface to volume ratio of the cardiac cells, $I_e$ is an extracellular current density stimulus, $C_m$ is the capacitance per unit area, and $I_{ion}$ is the current density flowing through the ionic channels. Eq. (2.1) is a parabolic equation and Eq. (2.2) is a set of ordinary differential equations which can be solved independently for each node. The transmembrane potential is defined by $V_m = \phi_i - \phi_e$, where $\phi_i$ and $\phi_e : Q_c \to \mathrm{R}$ are the intracellular and extracellular potentials.

Here the initial and boundary conditions are chosen as

$$(2.3) \qquad \bar{\sigma}_i \nabla V_m \cdot \eta = 0 \quad \text{on } \partial Q_c$$

$$(2.4) \qquad v(0) = v_0 \qquad \text{and} \quad V_m(0) = V_0 \quad \text{in } \Omega_c,$$

where $\partial Q_c = \partial \Omega_c \times [0, t_f]$.

**Ionic model.** The ionic activity is modeled by nonlinear ordinary differential equations. We refer to [14, 1, 8] for cell membrane models. For the present paper we use the modified Fitzhugh-Nagumo (FHN) model based on the work of Rogers and McCulloch and the simulation parameters are taken from Colli Franzone et.al [3].

$$(2.5) \qquad I_{ion}(V_m, v) = G V_m (1 - \frac{V_m}{v_{th}})(1 - \frac{V_m}{v_p}) + \eta_1 V_m v.$$

$$(2.6) \qquad g(V_m, v) = \eta_2 (\frac{V_m}{v_p} - \eta_3 v).$$

where $G, \eta_1, \eta_2, \eta_3$ are positive real coefficients, $v_{th}$ is a threshold potential and $v_p$ the peak potential.

**3. Optimal control problem .** Let $J$ denote the cost functional and consider the following PDE constrained optimal control problem,

$$(3.1) \qquad \begin{cases} \min J(V_m, I_e)\,, \\[2mm] e(V_m, v, I_e) = 0 \quad \text{in } Q_c\,, \end{cases}$$

where $V_m$ and $v$ denote the state variables, $I_e$ denotes the control variable and the coupled PDE and ODE, Eqs (2.1-2.2) is expressed as $e(V_m, v, I_e)$, with $e : V \times Y \times U \to W$. Here $V = H^1(\Omega_c)$, $Y = U = L^2(\Omega_c)$, $W = H^1(\Omega_c)^*$ and the $\Omega_c$ is an open bounded set in $\mathrm{R}^n$.

As a cost functional we choose by

$$(3.2) \qquad J(V_m, I_e) = \min \frac{1}{2} \int_0^T \left( \int_{\Omega_{obs}} |V_m|^2 \mathrm{d}\Omega_{obs} + \alpha \int_{\Omega_{con}} |I_e|^2 \mathrm{d}\Omega_{con} \right) dt\,,$$

where $\alpha$ is the weight of the cost of the control, $\Omega_{obs}$ is the observation domain and $\Omega_{con}$ is the control domain.

The Lagrangian related to the optimal control problem is given by

$$\begin{aligned} \mathcal{L}(V_m, v, I_e, p, q) &= J(V_m, I_e) \\ &+ \int_0^T \int_{\Omega_c} \left( \nabla \cdot \bar{\sigma}_i \nabla V_m - \beta \left( C_m \frac{\partial V_m}{\partial t} + I_{ion}(V_m, v) - I_e \right) \right) p \ \mathrm{d}\Omega_c \mathrm{d}t \\ (3.3) \qquad &+ \int_0^T \int_{\Omega_c} \left( \frac{\partial v}{\partial t} - g(V_m, v) \right) q \ \mathrm{d}\Omega_c \mathrm{d}t \end{aligned}$$

The first order optimality system is given by the Karusch-Kuhn-Tucker (KKT) conditions which result from equating the partial derivatives of $\mathcal{L}$ with respect to $V_m$ and $v$ in direction of $\delta x$ and $\delta y$ equal to zero:

$$(3.4) \qquad \mathcal{L}_{V_m}: \quad V_m + \nabla \cdot \bar{\sigma}_i \nabla p + \beta(C_m p_t - (I_{ion})_{V_m} p) - g_{V_m} q = 0\,,$$
$$(3.5) \qquad \mathcal{L}_v: \quad -\beta(I_{ion})_v p - q_t - g_v^T(V_m, v) q = 0\,,$$

where $(I_{ion})_{V_m}$ is the derivative of $(I_{ion})(V_m, v)$ w.r.t $V_m$ and $g_v^T(V_m, v)$ is derivative of the $g(V_m, v)$ w.r.t $v$.

$$(3.6) \qquad \text{Terminal conditions: } p(T) = 0\,, \qquad q(T) = 0\,.$$
$$(3.7) \qquad \text{Optimality conditions: } \mathcal{L}_{I_e}: \quad \alpha I_e + \beta p = 0\,, \quad \text{on } \Omega_{con}\,.$$
$$(3.8) \qquad \text{Boundary conditions: } \bar{\sigma}_i \nabla p \cdot \eta = 0 \quad \text{on } \partial Q_c\,.$$

Therefore, to solve (3.1) numerically we need to address the primal equations (2.1-2.2), the adjoint equations (3.4-3.5) the optimality and terminal conditions (3.6-3.7) together with initial and boundary conditions.

**3.1. Numerical approach.** The optimality system (2.1-2.2) and (3.4-3.5) is approximated by using a finite element method for the space discretization and linearly implicit Runge-Kutta methods for the time discretization.

**3.2. Space discretization using FEM.** In this subsection we give the brief introduction of a finite element method to solve the monodomain model equations. We will first consider a so-called *semi-discrete* analogue of the full system where we have discretized in space using the standard finite element method with piecewise bilinear continuous elements. Let $V_h \subset V$ be finite dimensional subspace and approximate the solution using the basis functions $\{w_i\}_{i=1}^N$. Finally, we get a system of ordinary differential equations in matrix form:

$$(3.9) \qquad -\mathbf{A_i V_m} = \beta \left( C_m \mathbf{M} \frac{\partial \mathbf{V_m}}{\partial t} + \mathbf{I_{ion}}(\mathbf{V_m}, \mathbf{v}) - \mathbf{I_e} \right),$$

$$(3.10) \qquad \frac{\partial \mathbf{v}}{\partial t} = \mathbf{g}(\mathbf{V_m}, \mathbf{v}),$$

$$(3.11) \qquad \mathbf{V_m}(0) = \mathbf{0}, \quad \mathbf{v}(0) = \mathbf{0}.$$

where $\mathbf{A_i}$ is the stiffness matrix and $\mathbf{M}$ is the mass matrix.

Here $\mathbf{I_{ion}}$ and $\mathbf{I_e}$ are vectors defined by $\mathbf{I_{ion}}(\mathbf{V_m}, \mathbf{v}) = \{\langle I_{ion}, w_j \rangle\}_{j=1}^N$ and $\mathbf{I_e} = \{\langle I_e, w_j \rangle\}_{j=1}^N$ respectively.

**Space discretization of dual problem.** We follow the analogous derivation like the primal problem and finally we obtain the system of ordinary differential equations in the following form.

$$(3.12) \qquad \mathbf{M V_m} - \mathbf{A_i p} = -\beta \left( C_m \mathbf{M} \frac{\partial \mathbf{p}}{\partial t} - \mathbf{M}(\mathbf{I_{ion}})_{\mathbf{V_m}} \mathbf{p} \right) + \mathbf{M} \mathbf{q} g_{V_m},$$

$$(3.13) \qquad \frac{\partial \mathbf{q}}{\partial t} = -g_v^T(V_m, v)\mathbf{q} - \beta (I_{ion})_v \mathbf{p},$$

$$(3.14) \qquad \mathbf{p}(T) = \mathbf{0}, \quad \mathbf{q}(T) = \mathbf{0}.$$

While solving the primal and dual problem, we first approximate the ODE system solution at current time step, which gives the ionic current variable update, and then stick this solution in the PDE. Finally, the PDE solution is approximated at the current time step using the current update for the ionic current variable. For more details we refer to our forth coming paper [9].

**3.3. Time discretization using linearly implicit RK methods.** In this subsection we give a brief introduction to the time discretization for solving the ordinary differential equation system which arises from the space discretization of the primal and dual equations. The ordinary differential equation system, acquired from the semi discretization in space is solved numerically with the finite difference method. We can write the ODE system in the following form:

$$(3.15) \qquad \mathbf{M} \frac{\partial \mathbf{u}}{\partial t} = \mathbf{F}(\mathbf{u}), \qquad \mathbf{u}(t^0) = \mathbf{u^0}.$$

To solve this system, we partition the time $[0, T]$ into discrete steps $0 = t^0, t^1, \dots, t^n = T$, which that are not necessarily equidistant. The notation for time step is $\tau^i = t^{i+1} - t^i$ and $\mathbf{u}^i$ is the numerical solution at time $t^i$. For the time discretization we used a linearly implicit Runge-Kutta methods, especially Rosenbrock methods. Rosenbrock methods belong to a large class of methods which try to avoid nonlinear systems and replace them by a sequence of linear systems. For our computations we used the *ROS2* method which has two internal stages to solve in each iteration, see [7] for more details. After the time discretization one ends up with system of

linear equations. For solving the linear system the BiCGSTAB method with ILU preconditioning is used in our computations.

In the optimization algorithm, the nonlinear conjugate gradient method and Newton's method are adopted to solve the optimality system, see [11] for more details. A more in depth description will be found in [9, 6]. The numerical realization has been carried out using the public domain package DUNE [2].

**4. Second order methods.** Aiming for a second order optimization algorithm, it is clear that due to problem size it is unfeasible to construct the true Hessian of the cost functional of the optimal control problem. Alternatives, based on model reduction or reduced storage techniques are conceivable. Here we explain the computation of the action of the "Hessian of reduced cost", which is a useful technique to solve the system without storing the Hessian in Newton's method. In our computations we use such techniques to solve efficiently the optimal control problems.

First we give a brief introduction of the main ingredients which are important to compute the action of the Hessian of the reduced cost. We denote $X = V \times Y$ and $u = (V_m, v)$ for $(V_m, v) \in V \times Y$. The non linear mapping $e : X \times U \to W$ can be written in the following form,

$$(4.1) \qquad e(V_m, v, I_e) = \begin{pmatrix} \nabla \cdot (\bar{\sigma}_i \nabla V_m) - \beta(C_m \frac{\partial V_m}{\partial t} + I_{ion}(V_m, v) - I_e) \\ \\ \frac{\partial v}{\partial t} - g(V_m, v) \end{pmatrix}$$

We refer to Hinze and Kunisch [5] for the formalism to compute the reduced Hessian of $\hat{J}(I_e) = J(V_m(I_e), I_e)$, where it is derived in the context of optimal control of the Navier-Stokes equations.

**Newton's method.** The linearisation of $e, I_{ion}$ and $g$, integrated with homogeneous initial and boundary conditions are given by :

$$(4.2) \qquad e_u(\delta V_m, \delta v) = \begin{pmatrix} \nabla \cdot (\bar{\sigma}_i \nabla \delta V_m) - \beta \left( C_m \delta V_{m_t} + \nabla I_{ion}(\delta V_m, \delta v) \right) \\ \delta v_t - \nabla g(\delta V_m, \delta v) \end{pmatrix}$$

where

$$(I_{ion})_{V_m}(\delta V_m, v) = G\delta V_m \left[ (1 - \frac{V_m}{v_{th}})(1 - \frac{V_m}{v_p}) - \frac{V_m}{v_{th}}(1 - \frac{V_m}{v_p}) - \frac{V_m}{v_p}(1 - \frac{V_m}{v_{th}}) \right]$$
$$+ \eta_1 \delta V_m v$$
$$(I_{ion})_v(V_m, \delta v) = \eta_1 V_m \delta v \,,$$
$$(4.3) \quad g_{V_m}(\delta V_m, v) = \eta_2 \frac{\delta V_m}{v_p} \,, \qquad g_v(V_m, \delta v) = -\eta_2 \eta_3 \delta v$$

Now the matrix operator $T(x)\delta I$ is computed as

$$(4.4) \qquad T(x)\delta I = \begin{pmatrix} -[\nabla e(V_m, v, I_e)]^{-1} \begin{pmatrix} \beta \delta I_e \\ 0 \end{pmatrix} \\ Id_{I_e} \end{pmatrix} =: \begin{pmatrix} \begin{pmatrix} \delta V_m \\ \delta v \end{pmatrix} \\ Id_{I_e} \end{pmatrix}$$

where $\nabla = \nabla_{V_m, v}$. The form of the second derivative of $\mathcal{L}$ is found to be

$$\nabla^2_{(V_m, v, I_e)} \mathcal{L}(V_l, v_l, \delta I) = \begin{pmatrix} \begin{pmatrix} -\Delta V_l - \beta(I_{ion})_{V_m V_m}(V_l)q - \beta \eta_1 v_l q \\ -\beta \eta_1 V_l q \\ \alpha \delta I \end{pmatrix} \end{pmatrix}$$

$$(4.5) \qquad\qquad =: \left( \begin{pmatrix} z_1 \\ z_2 \\ \alpha\delta I \end{pmatrix} \right)$$

$$(4.6) \qquad \text{where} \qquad (I_{ion})_{V_m V_m}(V_l) = 6G\frac{V_m V_l}{v_{th} v_p} - 2GV_l(\frac{1}{v_p} + \frac{1}{v_{th}}).$$

Finally, the computation of the action of Hessian can be expressed as

$$(4.7) \qquad\qquad (T^* \nabla^2 \mathcal{L} T)\delta I = -e_{I_e}^*(e_{(V_m,v)}^{-1})^* \begin{pmatrix} z_1 \\ z_2 \end{pmatrix} + \alpha\delta I$$

$$(4.8) \qquad\qquad\qquad = -\beta w_1 + \alpha\delta I$$

and the Newton system becomes

$$(4.9) \qquad\qquad (T^* \nabla^2 \mathcal{L} T)\delta I = -\hat{J}'(I_e^n).$$

where $\hat{J}'(I_e^n)$ is the gradient of the reduced cost functional $J(V_m(I_e), I_e)$. To solve (4.9) numerically an iterative algorithm like a CG method is used. To carry out a Newton step (without line search) the following algorithm is used. Here we summarize the basic steps to compute the action of Hessian, see [6] for more details.

1. Compute the $\hat{J}'(I^n)$ obtained by one solve of the primal and dual equations.
2. Iteratively solve (4.9). In each step the action of $\hat{J}'(I^n)$ on a direction $\delta I^n$ has to be evaluated by means of
   (a) solve the linearized primal equation for $V_l, v_l$ using $\delta I_j^k$.
   (b) evaluate the $(z_1, z_2)$ from eq. (4.5).
   (c) solve the adjoint equation with $(z_1, z_2)$ as r.h.s from eq. (4.7).
   (d) finally compute the action of $\hat{J}''(I^k)$ on $\delta I_j^k$ using eq. (4.8)

In practice the algorithm is combined with a line search strategy.

**5. Numerical results.** In this section we present the numerical results based on the first order method, namely on a nonlinear conjugate gradient method, and a second order method, Newton's method. The numerical results are shown for two test cases in solving short time horizon problems. The first one involves a tracking type cost functional and serves as a partial validation for the numerical procedure that we follow. The second one shows the capability of dampening an excitation wave of the transmembrane potential by properly applying an extracellular potential. The domain $\Omega_c = [0,1] \times [0,1]$ and various relevant subdomains are depicted in Figure 5.1. Here $\Omega_c$ denotes the computational domain, the observation domain is $\Omega_{obs} = \Omega_c \backslash \Omega_f$, the excitation domain is $\Omega_{exi}$ and the control domain is $\Omega_{con}$.

For the computations a uniform rectangular mesh and equidistant time steps are used. The computational mesh comprises of 2500 nodal points and 2401 quadrilateral elements. In all simulations the weight of the cost of the control ($\alpha$) is fixed at $\alpha = 10^{-3}$ and the iterations were terminated when the following condition is satisfied:

$$\|\nabla J_k\|_\infty \leq 10^{-3}(1 + |J_k|).$$

If this condition is not met within a 1000 iterations, then we terminate the optimization loop.

**Parameters used in the simulation.** $\sigma_{il} = 0.174$, $\sigma_{it} = 0.019$, $\sigma_{el} = 0.625$, $\sigma_{et} = 0.236$ $mS/cm$, $G = 1.5$ $mS/cm^2$, $v_{th} = 13$ $mV$, $v_p = 100$ $mV$, $\eta_1 = 4.4$ $mS/cm^2$, $\eta_2 = 0.012$, $\eta_3 = 1$, $\beta = 1000$ $cm^{-1}$, $C_m = 10^{-3}$ $mF/cm^2$.
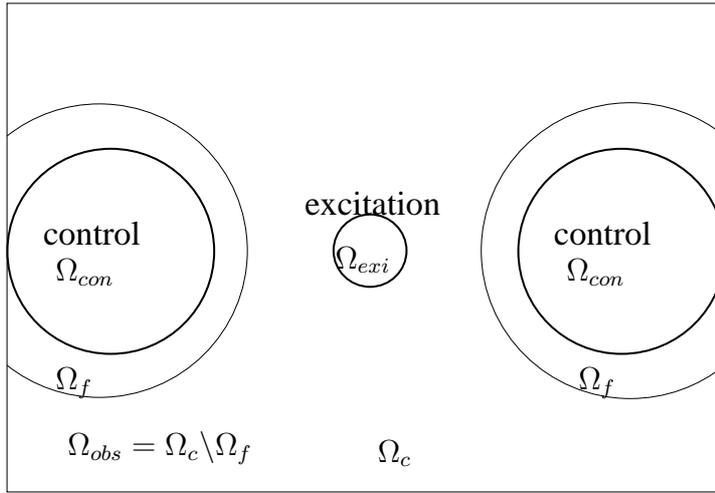
FIG. 5.1. *Control and excitation region at the cardiac domain*

**Test case 1.** In this case the tracking type cost functional

$$(5.1) \quad J(V_m, I_e) = \min \frac{1}{2} \int_0^T \left( \int_{\Omega_{obs}} |V_m - V_d|^2 \mathrm{d}\Omega_{obs} + \alpha \int_{\Omega_{con}} |I_e|^2 \mathrm{d}\Omega_{con} \right) dt,$$

where $V_d$ is the given desired state. Note that (5.1) represents the regularized least squares formulation of recovering the "true" $I_e$ from data $V_d$. Regularization, i.e. $\alpha > 0$, is required since the mapping $I_e \to V_m$ cannot be expected to have a continuous inverse. Using an initialization $(I_e)_0$ for NCG and Newton's methods different from the "true" $I_e$ we expect to recover $I_e$ up to the effect due to the regularization term.

The desired trajectory $(V_d)$ of the transmembrane voltage solution is computed as the solution to Eq. (2.1) using the excitation of the wave front at the excitation domain and turning on the extracellular current variable at the control domain in the model equations. Throughout this test case we use as initial conditions:

$$V_d(0) = \begin{cases} 105.0 & \text{in} \quad \Omega_{exi} \\ 0 & \text{otherwise} \end{cases}$$

$$(5.2) \qquad\qquad\qquad v(0) = 0 \quad \text{in } \Omega_c.$$

$$(5.3) \qquad\qquad\qquad I_e = \begin{cases} 15 & \text{in} \quad \Omega_{con} \times [0, T] \\ 0 & \text{otherwise}. \end{cases}$$

For globalization, first experiments were based on a strong Wolfe conditions with back tracking. However, in many cases it turned out to be computationally less efficient than the use of a fixed step length. It is chosen to be 0.3 for all results presented for Test case 1.

The algorithm is initialized by $(I_e)_0 = 0.75 \in \Omega_{con}$ and $(I_e)_0 = 0 \in \Omega_c \backslash \Omega_{con}$. The continuous $L^2$ norm of the gradient of the cost functional and the minimum value of the cost functional are depicted in Figure 5.2 and the corresponding minimum values of $\int |V_m - V_d|^2 \mathrm{d}x \mathrm{d}t$ and $\int |I_e|^2 \mathrm{d}x \mathrm{d}t$ are depicted in Figure 5.3 for different methods. For all methods the norm of the gradient decreases much more rapidly at the beginning than towards the end. In this case the NCG method with switching to
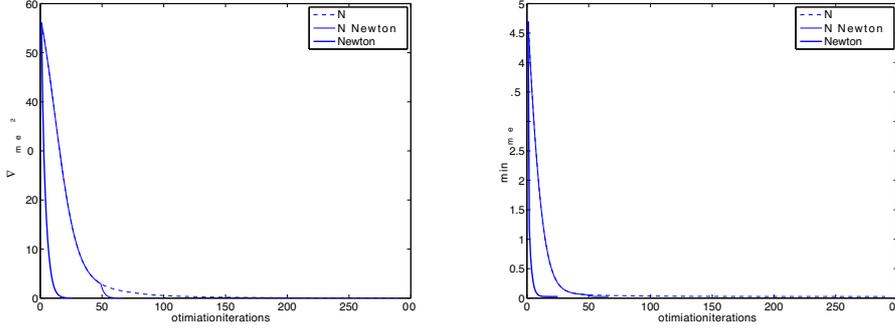
FIG. 5.2. *The norm of the gradient and minimum value of the cost functional are shown on left and right respectively for $T = 1$ msec of simulation time.*
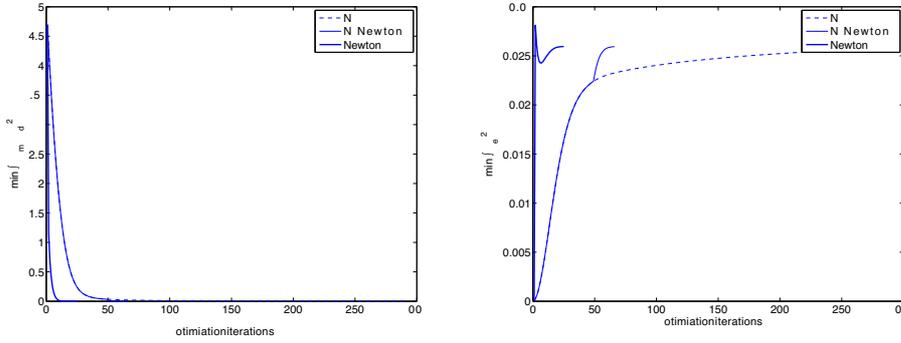


FIG. 5.3. *The minimum value of $\int |V_m - V_d|^2 \, dx \, dt$ and $\int |I_e|^2 \, dx \, dt$ is at left and right respectively for $T = 1$ msec of simulation time.*

Newton method takes 375.711 sec of CPU time and 67 optimization iterations (first 50 optimization iterations for the NCG method and subsequently 17 optimization iterations all together for the Newton's method). We observed that the switching from NCG to Newton's method takes less CPU time than the NCG and Newton's methods. The Newton's method takes 1.093 times the CPU time and the NCG method takes 1.7137 times the CPU time of the switching method. The Newton's method requires 26 optimization iterations and the NCG method takes 291 optimization iterations.

**Test case 2.** In this case the cost functional is minimized with respect to the transmembrane voltage in the observation domain and the extracellular current density as control variable in the control domain:

$$(5.4) \qquad J(V_m, I_e) = \min \frac{1}{2} \int_0^T \left( \int_{\Omega_{obs}} |V_m|^2 \, d\Omega_{obs} + \alpha \int_{\Omega_{co`n}} |I_e|^2 \, d\Omega_{con} \right) dt$$

The initial solution is considered for Test case 2 as follows:

$$V_m(0) = \begin{cases} 105.0 & \text{in} \quad \Omega_{exi} \\ 0 & \text{otherwise} \end{cases}$$

$$v(0) = 0 \quad \text{in } \Omega_c. \qquad (I_e)_0 = 0 \quad \text{in } \Omega_{con} \times [0, T].$$

For this simulation the step length is chosen to be 0.8 for all methods. The control variable on the control domain is initialized by $(I_e)_0 = 0$ in $\Omega_{con} \times [0, T]$. Further $I_e$ is set 0 on $\Omega_c \backslash \Omega_{con} \times [0, T]$. The continuous $L^2$ norm of the gradient and the minimum value of the cost functional for $T = 1$ msec of simulation time are presented in Figure 5.4. On this short time interval the control is not sufficient to dampen out the excitation wave. The norm of the gradient decreases much more rapidly at the beginning of the iterations than towards the end. The corresponding minimum values of $\int |V_m|^2 \mathrm{d}x\mathrm{d}t$ and $\int |I_e|^2 \mathrm{d}x\mathrm{d}t$ are depicted in Figure 5.5. In this simulation the Newton method takes 113 iterations to converge the prescribed tolerance in the optimization algorithm. While switching from NCG to Newton's methods takes 160 iterations and NCG method takes 641 iterations. The Newton's method takes fewer iterations than the other two methods. The NCG method takes 1351 sec of CPU time. The Newton's method is 1.059 times slower and the switching method is 1.143 slower than the NCG method for this particular case. The convergence factor for the Newton
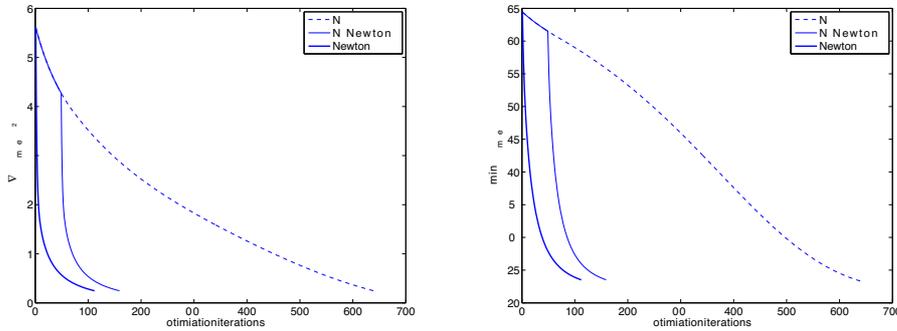


FIG. 5.4. *The norm of the gradient and minimum value of the cost functional are shown on left and right respectively for $T = 1$ msec of simulation time.*
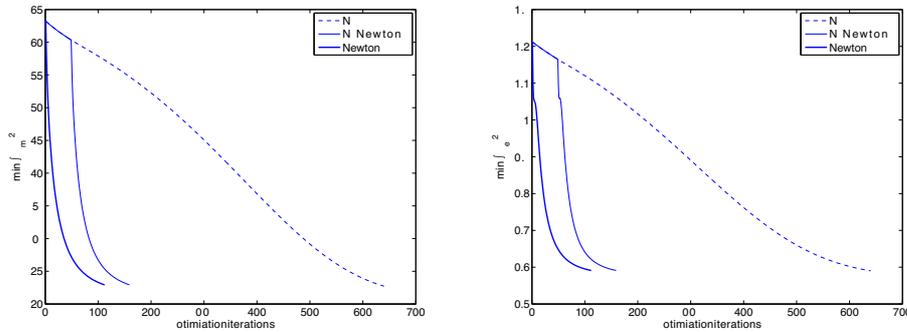


FIG. 5.5. *The minimum value of $\int |V_m|^2 dx dt$ and $\int |I_e|^2 dx dt$ is at left and right respectively for $T = 1$ msec of simulation time.*

method is smaller than the NCG method. To further improve the convergence factor for the Newton method the globalization strategy must be improved.

**6. Conclusions.** In this current article, second order methods for optimal control of the action potential in cardiac electrophysiology based on the monodomain

equation were discussed and numerical results for two selected test cases were presented. While the first test case provides validation of the numerical results, the second addresses the dampening of a wave front by properly applying extracellular currents. The second order methods are faster to converge to the solutions. Specifically, for this problem both the NCG and the Newton method are suitable for short time horizons. For long time horizons, the Newton method shows a clear improvement in convergence over the NCG method, see [6] for more details. Also, switching from NCG to Newton method also shows good improvement for some particular simulations. These results motivate us to continue our investigations for the bidomain model. The computational results, with extracellular control dampening the complete wave propagation of the transmembrane potential, suggest to strive for more insight into longer time horizons, with complete simulations of several heart beats, with more realistic geometries and finer meshes.

## REFERENCES

[1] Rubin R. Aliev and Alexander V. Panfilov. A simple two-variable model of cardiac excitation. *Chaos, Solitons & Fractals*, 7(3):293–301, Mar 1996.

[2] P. Bastian, M. Blatt, A. Dedner, C. Engwer, R. Klöfkorn, R. Kornhuber, M. Ohlberger, and O. Sander. A generic grid interface for parallel and adaptive scientific computing. part ii: implementation and tests in dune. *Computing*, 82(2):121–138, July 2008.

[3] P. Colli Franzone, P. Deuflhard, B. Erdmann, J. Lang, and L. F. Pavarino. Adaptivity in space and time for reaction-diffusion systems in electrocardiology. *SIAM Journal on Numerical Analysis*, 28(3):942–962, 2006.

[4] C. S. Henriquez. Simulating the electrical behavior of cardiac tissue using the bidomain model. *Crit. Rev. Biomed. Eng.*, 21:1 77, 1993.

[5] Michael Hinze and Karl Kunisch. Second order methods for optimal control of time-dependent fluid flow. *SIAM J. Control Optim.*, 40(3):925–946, 2001.

[6] K. Kunisch and Ch. Nagaiah. Second order numerical solution for optimal control of reaction-diffusion systems in cardiac electrophysiology. *preparation*.

[7] J. Lang. *Adaptive Multilevel Solution of Nonlinear Parabolic PDE Systems*, volume 16 of *Lecture Notes in Computational Science and Engineering*. Springer-Verlag, Berlin, 2001.

[8] C. Luo and Y. Rudy. A model of the ventricular cardiac action potential: Depolarization, repolarization, and their interaction. *Circ. Res.*, 68:1501–1526, 1991.

[9] Ch. Nagaiah, K. Kunisch, and G. Plank. Numerical solution for optimal control of mono-domain equations in cardiac electrophysiology. *submitted*.

[10] Bjørn Fredrik Nielsen, Tomas Syrstad Ruud, Glenn Terje Lines, and Aslak Tveito. Optimal monodomain approximations of the bidomain equations. *Applied Mathematics and Computation*, 184(2):276–290, 2007.

[11] J. Nocedal and S. J. Wright. *Numerical Optimization*. Springer Verlag, New York, second edition edition, 2006.

[12] R. Plonsey. Bioelectric sources arising in excitable fibers (alza lecture). *Ann. Biomed. Eng.*, 16:519 546, 1988.

[13] M. Potse, B. Dube, J. Richer, A. Vinet, and R.M. Gulrajani. A comparison of monodomain and bidomain reaction-diffusion models for action potential propagation in the human heart. *Biomedical Engineering, IEEE Transactions on*, 53(12):2425–2435, Dec. 2006.

[14] J. M. Rogers and A. D. McCulloch. A collocation-galerkin finite element model of cardiac action potential propagation. *IEEE Trans. Biomed. Eng.*, 41:743–757, 1994.